Mon. Not. R. Astron. Soc. **000**, 000–000 (0000) Printed 1 February 2008 (MN LATEX style file v1.4)

arXiv:astro-ph/9904056v1 5 Apr 1999

A deep search for pulsar wind nebulae using pulsar gating

B. W. Stappers[1]⋆, B. M. Gaensler[2,3,4,6], S. Johnston[5]
[1] *Sterrenkundig Instituut, Universiteit van Amsterdam, Kruislaan 403,1098 SJ Amsterdam, The Netherlands.*
[2] *Astrophysics Department, School of Physics A29, University of Sydney, NSW 2006, Australia.*
[3] *Australia Telescope National Facility, CSIRO, PO Box 76, Epping, NSW 2121, Australia.*
[4] *Center for Space Research, Massachusetts Institute of Technology, 70 Vassar Street, Cambridge, MA 02139, United States of America.*
[5] *Research Centre for Theoretical Astrophysics, University of Sydney, NSW 2006, Australia.*
[6] *Hubble Fellow.*

1 February 2008

ABSTRACT

Using the Australia Telescope Compact Array (ATCA) we have imaged the fields around five promising pulsar candidates to search for radio pulsar wind nebulae (PWNe). We have used the ATCA in its pulsar gating mode; this enables an image to be formed containing only off-pulse visibilities, thereby dramatically improving the sensitivity to any underlying PWN. Data from the Molonglo Observatory Synthesis Telescope were also used to provide sensitivity on larger spatial scales. This survey found a faint new PWN around PSR B0906–49; here we report on non-detections of PWNe towards PSRs B1046−58, B1055−52, B1610−50 and J1105−6107. Our radio observations of the field around PSR B1055−52 argue against previous claims of an extended X-ray and radio PWNe associated with the pulsar. If these pulsars power unseen, compact radio PWN, upper limits on the radio flux indicate that less than 10^{-6} of their spin-down energy is used to power this emission. Alternatively PSR B1046−58 and PSR B1610−50 may have relativistic winds similar to other young pulsars and the unseen PWN is resolved and fainter than our surface brightness sensitivity threshold. We can then determine upper limits on the local ISM density of $2.2 \times 10^{-3}\,\mathrm{cm}^{-3}$ and $1 \times 10^{-2}\,\mathrm{cm}^{-3}$, respectively. Furthermore we constrain the spatial velocities of these pulsars to be less than $\sim$450 km s^{-1} and thus rule out the association of PSR B1610−50 with SNR G332.4+00.1 (Kes 32). Strong limits on the ratio of unpulsed to pulsed emission are also determined for three pulsars.

Key words:
ISM: general – pulsars: individual PSR J1105−6107, PSR B1046−58, PSR B1055−52, PSR B1610−50 – radio continuum: ISM

1 INTRODUCTION

The majority of the spin-down energy $\dot{E}$ of a pulsar is carried away by a relativistic wind which is a combination of Poynting and kinetic-energy flux (Rees & Gunn 1974; Michel 1982). The exact contributions to the wind from the magnetic and particulate components is uncertain and has only been determined for the Crab (Kennel & Coroniti 1984) and PSR B1957+20 (Kulkarni et al. 1992). In contrast, the characteristic coherent pulsed radio emission represents only a small fraction of the total energy liberated.

Particles emerging from a pulsar magnetosphere have a null pitch angle and thus the relativistic wind is not directly observable. However, at a shock interface these pitch angles are randomised and produce synchrotron emission providing an excellent diagnostic of the wind (e.g. Frail et al. 1996). In the Crab Nebula the pulsar's wind is confined in the high pressure environment of the (invisible) surrounding supernova remnant (SNR) and a compact "plerion" is observed (Weiler & Panagia 1978). Outside this high-pressure environment, the pulsar wind experiences the much lower pressure of the general interstellar medium (ISM). This is expected to result in the formation of very large "ghost remnants" (Blandford et al. 1973), an example of which is yet to be discovered (Cohen et al. 1983). However, if the ram pressure resulting from the motion of the pulsar relative to the ISM is high, the interaction with the ambient medium may take the form of a bow-shock nebula. These nebulae are collectively known as pulsar wind nebulae (PWNe). Examples of plerions and bow-shock nebulae have been observed via

⋆ email : bws@astro.uva.nl

© 0000 RAS

Table 1. Summary of the sample pulsars' parameters

PSR	l (°)	b (°)	Period (ms)	τ_c (kyrs)	$\dot{E}$ (10^{34} erg s^{-1})	DM (pc cm^{-3})	Distance (kpc)
B1046–58	287.43	+0.58	124	20	200	129	3.0
B1055–52	285.98	+6.65	197	535	3	30	1.5
J1105–6107	290.49	–0.85	63	63	247	270	7.0
B1610–50	332.20	+0.18	232	7	160	582	7.2

their emission at optical (Hα) (e.g. Kulkarni & Hester 1988; Bell, Bailes & Bessell 1993), radio (e.g. Frail et al. 1996), and X-ray (e.g. Wang, Li & Begelman 1993) wavelengths. In general their radio emission is distinguished by having a flat spectral index and significant linear polarization. At present radio nebulae associated with pulsars are rare, with only seven examples known.

Discovering more PWNe which emit at radio wavelengths is of great interest. The spectral, polarization and energy properties of such nebulae provide us with valuable information on the energy and particle composition of the wind, the local ambient ISM density and the nebular magnetic field. For a bow-shock nebula the cometary morphology and associated trail can constrain both the transverse velocity of the pulsar and the direction of that motion. This may be critical when considering possible SNR associations where the pulsar is outside the remnant.

This paper reports on a search for radio PWNe around five southern pulsars. It was partially inspired by the present sparsity of radio PWNe and also by the recent VLA survey for PWNe carried out by Frail & Scharringhausen (1997, hereafter FS97). Their source list was made up of 35 candidates chosen for their high space velocity and/or high $\dot{E}$. To avoid contamination of a possible PWN by the pulsar itself they decided to observe at 3 cm where the flatter spectrum of any PWN should cause it to dominate its associated pulsar. Unfortunately, however, FS97 detected no new nebulae in their search. As those radio PWN already observed have $\dot{E} > 10^{35}\,\mathrm{erg\,s^{-1}}$, while the majority of the pulsars searched had $\dot{E} < 10^{35}\,\mathrm{erg\,s^{-1}}$, FS97 concluded that only young, energetic pulsars produce radio-bright PWNe. However, their choice of observing frequency and array configuration meant they could not have detected PWNe larger than 20 arcsec, and also had poor sensitivity to low surface brightness emission on smaller scales. They also could not tell if unresolved emission corresponded to compact PWNe or just to the pulsar itself.

In this experiment, we have used pulsar gating on the Australia Telescope Compact Array (ATCA) to remove the pulsed emission. This allows us to detect compact PWNe "hidden" behind the pulsar itself. It also enables us to observe at lower frequencies and resolution, resulting in a significantly more sensitive search. Our 20 cm observations have a typical (1 σ) sensitivity of 70 μJy beam^{-1} at ∼12 arcsec resolution, compared to FS97's 40 μJy beam^{-1} at 0.8 arcsec. Hence, for a typical PWN spectral index $\alpha = -0.3$ ($S_\nu \propto \nu^\alpha$), we are able to detect a PWN of surface brightness 200 times fainter than could FS97. Our observations are also sensitive to PWNe on scales up to ∼3 arcmin, ∼80 times the size of the largest sources which FS97 could detect. These observations were supplemented by Molonglo Observatory Synthesis Telescope (MOST) observations at 36 cm allowing us to probe spatial scales up to 80 arcmin.

This search targetted five southern pulsars (PSR B0906−49, PSR B1046−58, PSR B1055−52, PSR J1105−6107, PSR B1610−50). A nebula associated with PSR B0906−49 was successfully detected and is discussed in detail by Gaensler et al. (1998). We here report non-detections of PWNe towards the remaining candidates. Candidate selection is discussed in Section 2, while in Section 3 we discuss the observations and the pulsar-gating mode which we employed. In Sections 4 and 5 we present our results and go on to consider the corresponding implications.

2 THE SAMPLE

Because the ATCA is an East-West synthesis telescope, an image of each pulsar requires a full 12-hour synthesis, and on a reasonable timescale it is not possible to undertake a survey on the scale of that made by FS97. We therefore chose our sample of 5 pulsars based on a combination of their characteristic age ($\tau_c = P/2\dot{P}$), $\dot{E}$, and reported detections of a PWN at other wavelengths. The characteristics of the four pulsars, including their Galactic longitude, l, and latitude, b, rotational period, characteristic age, $\dot{E}$, dispersion measure, and the distance implied by the dispersion measure (Taylor & Cordes 1993), are given in Table 1. We now consider each pulsar in detail.

2.1 PSR B1046−58

PSR B1046−58 was discovered in a high-frequency survey of the Galactic plane (Johnston et al. 1992). It is young, $\tau_c \approx 20$ kyr, and has the 11th highest $\dot{E}$ of all known pulsars. Despite its youthfulness it is not near any known SNR. Its high $\dot{E}$ and relative proximity (2.5±0.5 kpc, Johnston et al. 1996) mean that it ranks in the top 10 pulsars when considering the spin-down energy flux at the Earth. Thus, it is an excellent candidate for having detectable high-energy emission (e.g. Fierro 1995) and is indeed coincident with the *EGRET* source 2EG J1049-5847 (Nel et al. 1996) and pulsations have probably been detected (Kaspi et al. 1998). There is also X-ray emission in the direction of the pulsar which has been detected by both *ASCA* (Kawai & Tamura 1996; Kawai, Tamura & Saito 1998) and *ROSAT* (Becker & Trümper 1997). The *ASCA* results suggest that this emission is extended and may be from a pulsar-powered nebula.

Table 2. ATCA observations of PWN candidates.

Source	Date	Secondary Calibrator	$B_{\rm max}$ (m)	ν (GHz) 1	ν (GHz) 2	t_{res}[a] (ms)
B1046–58	1997 May 13	PKS B1215-457	5969	1.344	2.240	3.9
B1055–52	1997 May 14	PKS B1215-457	5969	1.344	2.240	6.2
J1105–6107	1995 June 1	PKS B1036-697	750	1.376	...	7.9
J1105–6107	1995 May 16	PKS B1036-697	1485	1.376	...	7.9
B1610–50	1997 May 10	MRC B1613-586	5969	1.344	2.496	8.0(7.2)

(a) The values in parentheses corresponds to the effective time resolution at 13 cm for PSR B1610−50. For all other pulsars it does not differ from the effective time resolution at 20 cm.

2.2 PSR B1055−52

PSR B1055−52 is not particularly young, energetic nor rapidly rotating. However it is one of only a small number of pulsars which are detected across the whole electromagnetic spectrum and one of only seven pulsars known to pulse in high-energy γ-rays. It is a bright X-ray source (Cheng & Helfand 1983) with the soft photons modulated at the pulse period (Ögelman & Finley 1993) and is the pulsar which converts the largest fraction of its spin-down energy into pulsed γ-ray emission (Thompson et al. 1999). Recent *HST* observations by Mignani, Caraveo & Bignami (1997) were successful in detecting the optical counterpart. The optical emission is consistent with thermal emission from the neutron star surface.

The *Einstein* detection of PSR B1055−52 showed an apparently resolved source, suggesting that the X-ray emission was from a PWN (Cheng & Helfand 1983). However *ROSAT* observations made by Ögelman & Finley (1993) indicate no extended structure. Subsequent *ASCA* observations in the 2–8 keV X-ray band show a clumpy 20 arcmin ring around the pulsar which has also been interpreted as a PWN (Shibata et al. 1997). Although not conclusive these X-ray results suggest PSR B1055−52 may be embedded in a PWN. Combi, Romero & Azcárate (1997) have searched for an associated radio PWN using a 30 m dish at 20 cm. They detected a $66' \times 126'$ radio source overlapping the pulsar's position and the proposed X-ray nebula. Comparing this emission with a similar structure they see in the 408 MHz (74 cm) all-sky survey of Haslam et al. (1982) they measured a non-thermal spectrum and suggested that the source may represent synchrotron emission from a PWN powered by PSR B1055−52.

2.3 PSR J1105−6107

PSR J1105−6107 is both young and energetic (Kaspi et al. 1997). Like PSR B1046−58 its high $\dot{E}$ suggests that it may be a γ-ray source and it is coincident with 2EG J1103–6106. However Kaspi et al. (1998) find no evidence for γ–ray pulsations attributable to PSR J1105−6107. This pulsar is also near the SNR G290.1–00.8 and an association has been proposed by Kaspi et al. (1997). For the age and distance given in Table 1, the association with G290.1–00.8 implies a projected velocity for the pulsar of $v_{\rm t} \approx 650\,{\rm km\,s^{-1}}$ in order to have reached its present location well outside the SNR. X-ray observations with *ASCA* indicate the presence of an unpulsed source at the pulsar's position which is interpreted as a PWN (Gotthelf & Kaspi 1998).

2.4 PSR B1610−50

PSR B1610−50 is the third youngest known pulsar in the Galaxy. Its youth suggests that it be associated with a SNR and indeed an association with the nearby SNR G332.4+00.1 (Kes 32) has been claimed by Caraveo (1993). The pulsar is ∼12 arcmin from the center of the SNR, so an association therefore requires a transverse velocity for the pulsar, $v_{\rm t} \approx 460 \times d_{\rm kpc}\,{\rm km\,s^{-1}}$, where $d_{\rm kpc}$ is the distance to the pulsar in kpc. Its distance is quite uncertain, but taking the minimum remnant/pulsar distance, $d_{\rm kpc} \sim 5$ (e.g. Johnston et al. 1995) gives a distinctly high implied velocity, $v_{\rm t} = 2300\,{\rm km\,s^{-1}}$. Such a large velocity should result in a large ram pressure with the ISM, and thus a radio-bright PWN with a cometary tail indicating the pulsar's motion might be expected (Frail & Kulkarni 1991). As is typical for a young pulsar, PSR B1610−50 shows excessive timing noise and glitches, and thus its position from pulse timing analysis is not well known (Johnston et al. 1995). However an added advantage of the gated observations used here is that the pulsar's position can be accurately determined.

3 OBSERVATIONS AND DATA REDUCTION

Observations made with the ATCA (Frater, Brooks & Whiteoak 1992) are described in detail in Table 2 where $B_{\rm max}$ is the maximum baseline and ν is the central observing frequency. Observations were made simultaneously at approximately 20 cm and 13 cm, except for PSR J1105−6107 for which only 20 cm data were obtained. A total bandwidth of 128 MHz, divided into 32 channels, and all Stokes parameters was recorded at both wavelengths. All observations used the ATCA's pulsar gating mode, which divides the visibilities into a maximum of 32 time bins per pulse period, with a minimum width of ∼2.5 ms. A polynomial description of the apparent pulse period is then used to fold these bins online. Summed visibilities were then recorded every 40 s. The more rapid rotation rate of PSR J1105−6107 meant that only 8 bins were used, while all 32 bins were recorded for the remaining pulsars. The effective time resolution, t_{res} for both frequencies is given in Table 2. The dispersion measure smearing inside each 4 MHz channel was less than or approximately equal to the sampling time in all cases except

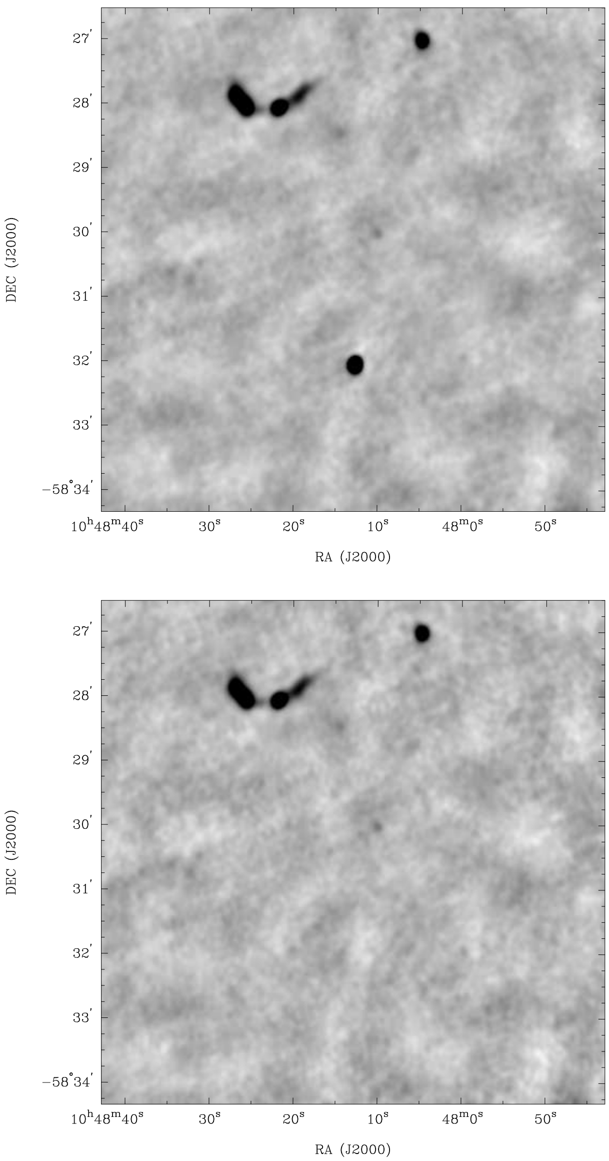

Figure 1. Two `CLEAN`ed images of the field around PSR B1046−58 are shown. Above all bins have been used; below only the off pulse bins are included. The ease of identification of any non-pulsed emission are immediately apparent. No PWN is discernible in the off-pulse image on any spatial scale, a conclusion which can only be drawn when pulsar gating is applied.

for PSR B1610−50 at 20 cm (both 20 cm and 13 cm resolutions for PSR B1610−50 are therefore given in Table 2). For PSR B1046−58, PSR B1055−52 and PSR B1610−50, the pulsar was offset from the phase center by a few arcminutes. Observations of PSR J1105−6107 were centered on the SNR G290.1–01.8, so that the pulsar was approximately 22 arcmin away from the field center.

For all sources the flux density scale was determined by observations of PKS B1934–638 using the revised flux density scale of Reynolds (1994). The antenna gains were determined by observations, every 40 minutes, of the secondary calibrators given in Table 2. Data reduction, including editing and calibrating, was carried out using the `MIRIAD` package and standard techniques (Sault & Killeen 1998). Once calibrated, the data were dedispersed to the center frequency of the observations using the dispersion measures (DMs) given in Table 1. An image of each field was made, deconvolved using the `CLEAN` algorithm (Clark 1980), and restored using a Gaussian beam with dimensions appropriate for the diffraction limit (see θ_{min} in Table 4) and finally a correction for primary beam attenuation was made.

Each pulsar was identified by subtracting, after dedispersion and appropriate scaling, an image made from the first bin alone from an image made using all bins. As the pulse was the only unique feature in any bin it is the only source in the image[†]. The pulsar's position was determined by fitting a point source to the on-pulse $u-v$ data, and the pulse profile was extracted from the entire data-set at that position. The off-pulse bins were used to re-image the field and generate an image which contained no pulsed emission. Any underlying PWN emission can then be identified. Fig. 1 compares the effect of using all bins when observing PSR B1046−58 (i.e. equivalent to observing without gating) with that of using only the off-pulse bins.

Our ATCA observations are only sensitive to a maximum spatial scale of ∼3 arcmin. To search for more extended structures we used data from the MOST (Robertson 1991), an East-West synthesis telescope operating at a fixed wavelength of 36 cm. The MOST images all spatial scales between 43 arcsec and ∼80 arcmin with a typical sensitivity (for a 12 h synthesis) of 1 mJy beam^{-1}, and is therefore particularly sensitive to large-scale structure. These observations did not use pulsar gating. Data from the MOST Galactic plane survey (Green et al. 1999) were used for PSR B1046−58, PSR J1105−6107 and PSR B1610−50, while a separate observation was made of PSR B1055−52 on 1998 Apr 4.

4 RESULTS: PULSED EMISSION

Pulsations from PSR B1046−58, PSR B1055−52 and PSR B1610−50 were successfully detected in our observations and their 20 cm pulse profiles are presented in Fig. 2. These profiles, within the limited resolution, are consistent with the known pulse shapes and similar profiles were obtained at 13 cm. In all cases the pulsed emission can be clearly separated from any off-pulse contribution. Flux densities and the interferometric positions for all three detected pulsars are given in Table 3.

The flux of PSR B1046−58 at 20 cm is consistent with that in the pulsar catalogue (Taylor et al. 1995), while PSR B1610−50 has a 20 cm flux approximately twice that given in the catalogue; no catalogue value for the 20 cm flux is given for PSR B1055−52. A confusing thermal source, discussed below, is located near the position of PSR J1105−6107 and prevented its detection. The sensitivity limit for detection was very close to the known 20 cm flux density of PSR J1105−6107, 1.8 mJy (Kaspi et al. 1997).

The position (Table 3) of PSR B1055−52 matches the

[†] Noting that if the strongest section of the pulse is in the first bin the pulsar will appear negative

Table 3. Observed parameters of the detected pulsars.[a]

Name	Interferometric Position		Flux Density (mJy)		
	R.A. (2000)	Dec. (2000)	36 cm	20 cm	13 cm
B1046–58	10:48:12.6(3)	-58:32:03.75(1)	10(3)	9.4(5)	7.0(1)
B1055–52	10:57:58.9(9)	-52:26:56.1(2)	15(2)	8.7(2)	3.5(1)
B1610–50	16:14:11.6(8)	-50:48:01.90(9)	...	4.7(2)	1.0(1)

(a) The values in parentheses correspond to the 1 σ errors in the final digit.

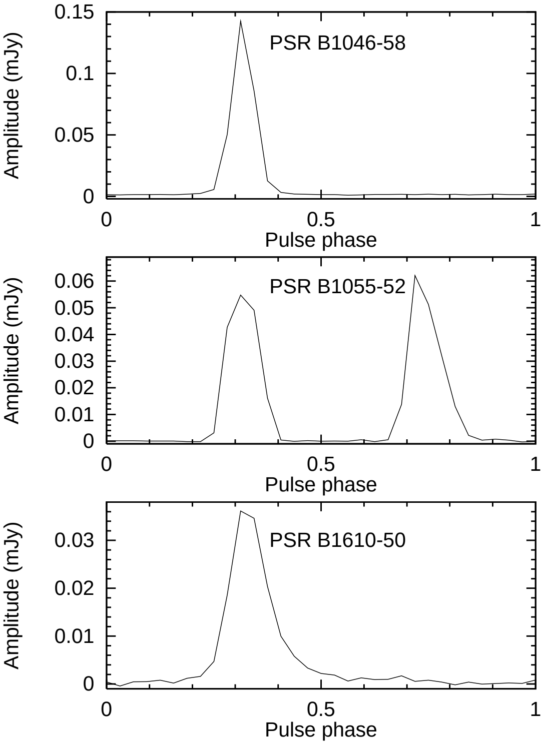

Figure 2. The 20 cm pulse profiles for the pulsars, as labelled, detected in these observations. Profiles at 13 cm looked similar. Thirty two time bins were used and the time resolution is given in Table 2. In all three cases there are sufficient off-pulse bins to generate a high signal-to-noise off-pulse map. Absolute timing was not carried out and the reported pulse phase is therefore arbitrary.

timing position to within the errors and our position for PSR B1046−58 is only ≈ 2.3 arcsec different in declination. The position of PSR B1610−50 is ill-determined from timing and our improved position, RA (J2000) $16^{\rm h}14^{\rm m}11\overset{\rm s}{.}6$, Dec (J2000) $-50^{\circ}48'01\overset{\prime\prime}{.}90$, is approximately half an arcminute away from the nominal timing position of Johnston et al. (1995).

5 RESULTS: OFF-PULSE EMISSION

No off-pulse emission, either extended or unresolved, was detected from any of the four pulsars discussed here. The 1 σ surface brightness limits, σ_{rms}, for these non-detections are given in Table 4. These limits are determined by measuring the rms variation in the off-pulse image in the vicinity of the pulsar. Also shown are the minimum, θ_{min}, and maximum, θ_{max}, angular scales to which we were sensitive at 20 cm. Two observations were made of PSR J1105−6107 one of which used a more compact configuration thereby increasing the angular size to which we were sensitive.

The lack of any unpulsed emission in the vicinity of PSR B1046−58 is starkly apparent in Fig. 1. The 5 σ limits for any undetected point-like nebula are 0.7 mJy and 0.4 mJy at 20 and 13 cm respectively.

Fig. 3 shows a 20 cm off-pulse image of the field surrounding PSR B1055−52 with the *ASCA* X-ray contours in the energy band 0.5–2.0 keV overlayed. The position of the pulsar is marked by the cross and the contours corresponding to the X-ray emission from the pulsar and the three "clumps" (Shibata et al. 1997) are clearly seen. There is no indication of any extended or point-like radio emission detected at the position of the pulsar. Radio emission is seen at the position of at least two of the three clumps, however it is clearly resolved into a number of discrete point sources and does not appear to form part of a large extended structure.

The location of PSR J1105−6107 relative to SNR G290.1–0.8 is indicated by the cross in the MOST 36 cm image in the left hand panel of Fig. 4. Similarly the pulsar is marked in the higher resolution 20 cm ATCA image of the immediate region around the pulsar's location. Neither of these images have been gated and the pulsar is undetected at both frequencies. An extended source, whose center is some 4 arcmin to the North of the pulsar, is clearly seen in the 20 cm image and is also detected at 36 cm. As this emission is diffuse and is coincident with an IRAS 60 μm source it is probably thermal and not associated with the pulsar. The pulsar is un-detected but the 5 σ limit on any possible PWN radio emission was only 1.5 mJy at 20 cm.

The 36 cm MOST image of the complicated field surrounding PSR B1610−50 is shown in Fig. 5. SNR Kes 32 is seen to the north-east while SNR G332.0+00.2 is to the south-west. Using our ATCA data we also show a higher resolution image of the region immediately surrounding the pulsar. After gating out the pulsar's emission we detect no unpulsed emission except for a filled-center clump located some 2 arcmin north of the pulsar which we designate G332.23+00.2. No linear polarization was detected from G332.23+00.2 and we measure flux densities of 0.20±0.05 Jy (36 cm) and 0.20±0.02 Jy (20 cm), suggesting a flat spectral index, while it was largely resolved out in our 13 cm observations.

Table 4. Limits on nebular and unpulsed flux densities.

Source	σ (mJy/beam) 36 cm	20 cm	13 cm	$\theta_{\rm min}$ ($''$)	$\theta_{\rm max}$ ($'$)	L$_{\rm R}$ (erg s^{-1})	L$_{\rm R}$/Ė (10^{-6})	$\sigma_{\rm off}$/S 20 cm	13 cm
B1046–58	0.8	0.14	0.08	10	3.2	3×10^{29}	0.15	0.015	0.011
B1055–52	1.2	0.08	0.16	10	3.2	4.5×10^{28}	1.5	0.009	0.05
J1105–6107	12	0.3	...	20	15.6	2.5×10^{30}	1.6	...	...
B1610–50	5.0	0.2	0.16	12	3.2	3.5×10^{30}	1.4	0.04	0.15

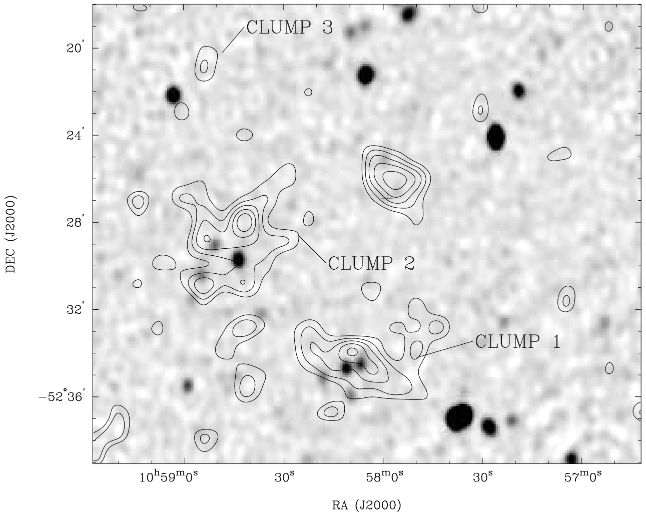

Figure 3. Radio and X-ray observations of PSR B1055−52. The grey-scale corresponds to a 20 cm off-pulse image, overlayed with X-ray contours from the *ASCA* 0.5–2 keV energy band. The X-ray contours are at 50%, 60%, 70%, 80% and 90% of the peak value. The position of the pulsar is labelled by the cross and the three clumps of Shibata et al. (1997) are indicated. The X-rays associated with the pulsar are clearly seen. There is no evidence for unpulsed radio emission at or around the position of the pulsar.

6 DISCUSSION

We have failed to detect any radio-bright PWNe emission over a wide range of angular scales and down to good sensitivities around PSRs B1046−58, B1055−52, J1105−6107 and B1610−50. These non-detections have interesting implications for all of these pulsars and we will consider them in detail below. Furthermore the gating method employed here also allows us to put a strong limit on the off-pulse emission from the pulsar itself. In Table 4 we give the limits on the ratio of the off-pulse rms noise to the on-pulse flux density. For PSR B1046−58 and PSR B1055−52 our limits are strong, and indicate that for these young pulsars any unpulsed radio emission from the neutron star itself is less than 2% of the pulsed emission (c.f. Hankins et al. 1993).

For PSR J1105−6107 and PSR B1610−50, we might have expected compact, ram-pressure confined PWNe, resulting from the high velocities inferred through associations with nearby SNRs. The emission from such nebulae may be located quite close to the termination shock radius, $r_{\rm s}$. For example we can derive an expression for the expected angular size of this shock (e.g. Cordes 1996) near PSR B1610−50 for a spherical wind;

$$\theta = \frac{0\farcs15}{d_7 v_{1000}}\sqrt{\frac{f}{n}}, \qquad (1)$$

where $v = v_{1000}\times1000\,{\rm km\,s^{-1}}$ is the pulsar's velocity, $d = d_7\times7\,$kpc is the distance, n is the density of the local ISM in cm^{-3} and f is the efficiency of conversion of spin-down energy to wind energy. Hence emission near $r_{\rm s}$ would be unresolved in our observations under the assumption of high-velocity.

In fact, if we assume that all the pulsars in our sample are moving with a typical pulsar velocity, $250\,{\rm km\,s^{-1}}$ (e.g. Hansen & Phinney 1997) and in ambient medium of density $n\approx0.1\,{\rm cm^{-3}}$, PWN around them will be unresolved in our 20 cm data. Similarly to FS97, using our non-detections we can then determine an upper limit on the radio luminosity, L$_{\rm R}$, for these compact nebulae. Assuming a Crab-like spectral index (noting that the spectral index of the PWN associated with PSR B0906−49 is steeper);

$$L_{\rm R} = 4.74\times10^{28}d_{kpc}^2S_{20}\,{\rm erg\,s^{-1}}, \qquad (2)$$

where $d_{\rm kpc}$ is the distance to the nebulae and S_{20} is the 20 cm flux limit.

The L$_{\rm R}$ for each non-detection, based on the $5\,\sigma$ limiting flux density at 20 cm, is given in Table 4. Comparing these maximum L$_{\rm R}$ values with the known $\dot{E}$ we find that the pulsars in our sample have efficiencies (see Table 4) which lie in or below the peak of the distribution shown by FS97 at L$_{\rm R}/\dot{E}\sim10^{-6}$. Thus for an unresolved nebula the efficiencies are well below those at which radio PWNe appear to be detected.

An alternative to this implied low efficiency for the lack of PWN could simply be the fact that the PWN are resolved but are too faint to see. Both PSR B1046−58 and PSR B1610−50 have similar ages, spin-down energies and surface magnetic fields to PSR B1757–24 (Frail et al. 1996) and PSR B1853+01 (Frail & Kulkarni 1991) which are known to have associated PWN. If we therefore assume that these pulsars all have similar wind characteristics and that conditions at the shock with the ISM are the same, then the ratio of the resultant PWN's radio luminosity to the spin-down energy should also be similar.

Using Equation 2, together with the distances and spin-down energies given in Table 1 and L$_{\rm R}/\dot{E}\sim2\times10^{-4}$ (e.g. PSR B1757–24; FS97), we find that PWN associated with PSR B1046−58 and PSR B1610−50 should have S$_{20}$ = 1 and 0.1 Jy respectively. To reconcile these expected flux densitys with the observed surface brightness limits these nebulae must be larger than a certain radius. Assuming circular nebulae with uniform surface brightness our $3\,\sigma$ flux-density

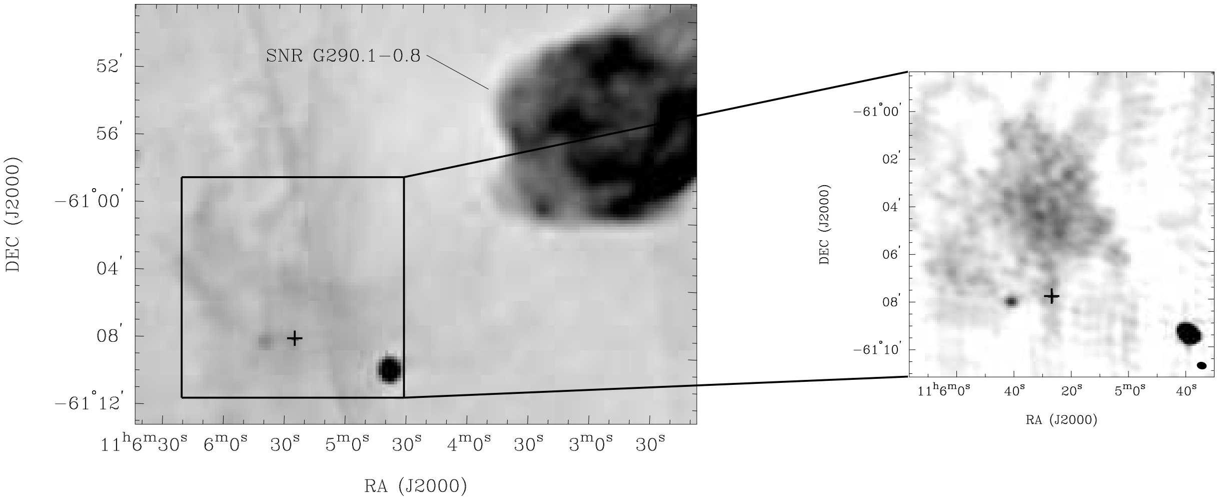

Figure 4. Radio observations of PSR J1105−6107. Left: A 36 cm MOST image of the field, including the SNR G290.1–0.8. Right: A higher resolution, 20 cm, ATCA image of the immediate region surrounding the pulsar. The ATCA synthesised beam is shown at lower right. No pulsar gating has been applied to either image, and the pulsar position is indicated by the cross. The thermal emission directly to the North of the pulsar can clearly be seen in the ATCA image.

limits correspond to PWNe of minimum radii 8 and 3 pc respectively[‡].

Now consider that this minimum radius corresponds to the radius of a static PWN (Arons1993);

$$R_s = \left(\frac{\dot{E}}{4\pi\rho_0}\right)^{1/5} t^{3/5}\text{cm}, \tag{3}$$

where ρ_0 is the density of the surrounding medium in $\mathrm{g\,cm^{-1}\,s^{-2}}$ and t is the age, we can derive a number density of the surrounding medium, n_0. Around PSR B1046−58 $n_0 \lesssim 2.2 \times 10^{-3}\,\mathrm{cm^{-3}}$ and for PSR B1610−50 $n_0 \lesssim 1.0 \times 10^{-2}\,\mathrm{cm^{-3}}$, where we have assumed a purely hydrogen ISM.

If instead we consider the case where the winds are in pressure balance at the aforementioned radii due to ram pressure then we find that $n_0 v^2 \lesssim 0.4\,\mathrm{cm^{-3}\,km^2\,s^{-2}}$ for PSR B1046−58 and $n_0 v^2 \lesssim 2\,\mathrm{cm^{-3}\,km^2\,s^{-2}}$ for PSR B1610−50. Thus for reasonable pulsar velocities the implied density of the ISM is exceptionally low and we conclude that these nebulae are probably not ram pressure confined. In this case the pulsar velocity, v, cannot be significantly greater than the ISM shock velocity and thus,

$$v \approx \dot{R}_S = \left(\frac{3}{5}\right)\left(\frac{\dot{E}}{\rho_0 t^2}\right)^{1/5} \mathrm{cm\,s^{-1}}. \tag{4}$$

Equating t to the characteristic age of the pulsar and using our limits on n_0 above, we obtain significant constraints on the maximum space velocity of PSR B1046−58 and PSR B1610−50 of $480\,\mathrm{km\,s^{-1}}$ and $450\,\mathrm{km\,s^{-1}}$, respectively.

6.1 PSR B1046−58

PSR B1046−58 is a young pulsar which we have shown is probably in a low density region which is consistent with it having no associated SNR. Located near the pulsar there is a 100 pc expanding gas shell centered on a pair of OB associations (Cowie et al. 1981). Johnston et al. (1996) speculate that this shell may be related to the SN which formed PSR B1046−58. It is therefore probable that despite being very energetic, PSR B1046−58 dwells in an environment which precludes the formation of a radio bright PWN.

6.2 PSR B1055−52

To properly compare our observations with the proposed extended nebula detected by Combi et al. (1997) we smoothed our data to ∼24 arcmin, the same resolution as their measurements. When smoothed, the distribution of point sources shown in Fig. 3 almost exactly reproduces the size and shape of the Combi et al. (1997) emission at 20 cm. Furthermore, the MOST data are sensitive to emission on scales as large as 80 arcmin, but show no evidence for extended radio emission. Thus we conclude that the source claimed as a PWN by Combi et al. (1997) is spurious, and is simply the effect of confusing sources observed with a small dish.

The proposed X-ray PWN associated with PSR B1055−52 is made of three clumps as indicated in Fig. 3. At least two of these three clumps coincide with clusterings of radio point sources seen in our 20 cm observations, and also with X-ray point sources seen in archival *ROSAT* data (Becker 1998). We thus think it more likely that the *ASCA* clumps correspond to emission from unrelated background sources, rather than to a PWN associated with PSR B1055−52.

To summarise, we argue that there is no evidence for either a radio or an extended X-ray PWN around PSR B1055−52. It may be that PSR B1055−52 is converting the

---

[‡] The MOST offered the best sensitivity limit for PSR B1046−58. Hence, assuming a Crab-like spectral index, the 20 cm flux limit was converted to a 36 cm flux limit for comparison with the MOST upper limit

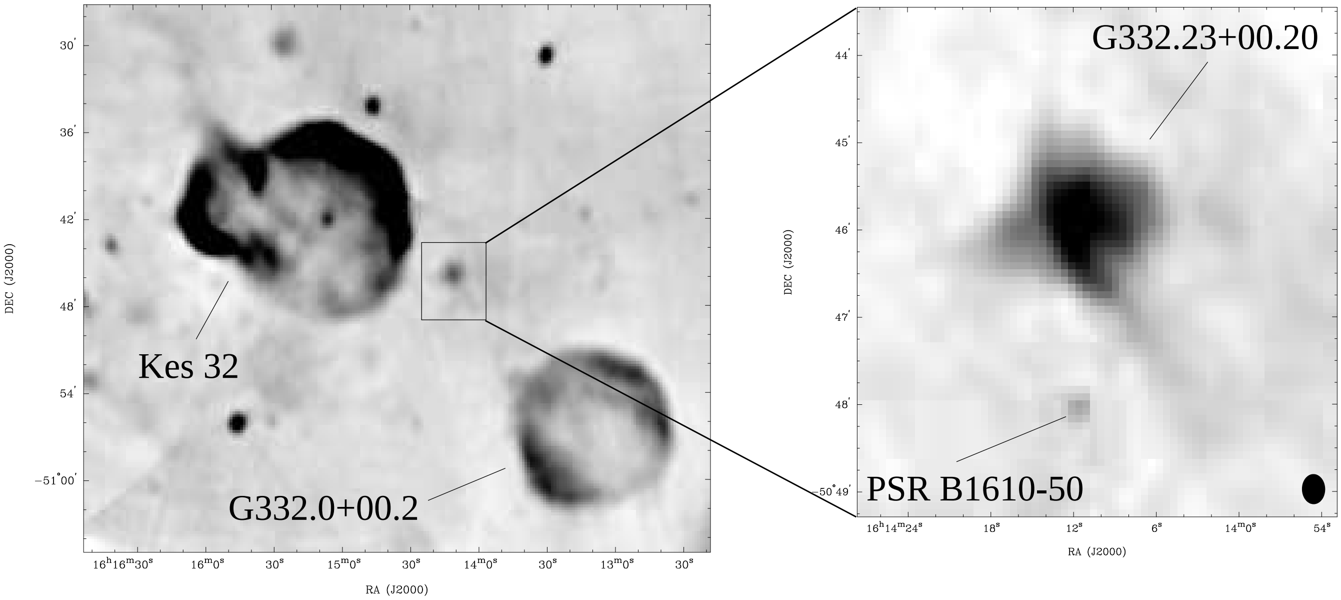

Figure 5. Radio observations of PSR B1610−50. Left: A 36 cm MOST image of the field, including the SNRs Kes 32 and G332.0+00.2. Right: A higher resolution, 20 cm, ATCA image of the immediate region surrounding the pulsar. This image was formed by combining our ATCA data with other, archival, observations of the region to give improved $u-v$ coverage and sensitivity. No pulsar gating has been applied to this image, and the pulsar is indicated. A knot of emission, G332.23+00.20, can be seen to the north. The ATCA synthesised beam is shown at lower right.

majority of its spin-down luminosity into high energy emission, rather than into a relativistic wind. PSR B1055−52 may emit as much as 21% (assuming emission into 1 steradian) of its spin-down energy at energies greater than 1 eV (Thompson et al. 1999) which is significantly more than for the other pulsars in our sample.

6.3 PSR J1105−6107

Extensive thermal emission in the vicinity of PSR J1105−6107 restricts the sensitivity limits which we can place on any potential radio PWN. If this thermal source is an H II region and lies along the line of sight to the pulsar then this may mean that the pulsar distance derived from its dispersion measure is significantly over-estimated. Extrapolating the power-law spectrum of the X-ray PWN ($\alpha = -0.8 \pm 0.4$; Gotthelf & Kaspi 1998) through to radio wavelengths, we find that we expect a 20 cm flux density for any radio PWN of ∼0.5 Jy. This corresponds to a $5\,\sigma$ detection of a ∼3 arcmin sized nebula in our 20 cm data. The expected radio flux falls below our detection threshold provided there is a break to a Crab-like spectrum ($\alpha = -0.3$) at a frequency above 10^{14} Hz.

6.4 PSR B1610−50

As shown in Fig. 5, the clump of emission G332.23+00.2 is quite close to the pulsar. While its filled-centre morphology and flat spectrum are what might be expected from a PWN, the pulsar is well outside this source and there is no morphological evidence to suggest the two are associated. Rather, the non-detection of linear polarization from G332.23+00.2 suggests that it is an unrelated thermal region. The presence of strong IRAS 60 μm emission nearby prevents a clear determination of whether G332.23+00.2 also emits at this wavelength.

The lack of a PWN associated with PSR B1610−50 indicates that the pulsar is located in a low-density environment and is moving with moderate velocity. The probability of a chance association along the line-of-sight to this pulsar is high, as this complex region contains several SNRs and pulsars (e.g. Johnston et al. 1995; Gaensler & Johnston 1995). Furthermore, unlike the case of PSR B1757–24 and G5.4-1.2 (Frail & Kulkarni 1991), there is no evidence of disruption of the SNR where the pulsar would have passed through the shell. From consideration of all these points, we strongly argue that the association by Caraveo (1993) of PSR B1610−50 with Kes 32 is inconsistent with our data.

Thus, even though PSR B1610−50 is a very young pulsar, there are no obvious SNRs with which it might be associated. We do not consider this a problem, however, we believe it to be located in a medium with density $n_0 \lesssim 1.0 \times 10^{-2}\,\mathrm{cm}^{-3}$ and since a large fraction of the ISM is believed to consist of low density coronal gas (e.g. McKee & Ostriker 1977), SNRs expanding into such regions will be undetectable (e.g. Kafatos et al. 1980).

7 CONCLUSIONS

Using the excellent sensitivity to unresolved nebulae afforded by the gating mode of the ATCA and the greater spatial sensitivity of the MOST we have searched for PWNe around five pulsars. We successfully detected a new nebula associated with PSR B0906−49 and failed to detect any extended or unresolved nebulae associated with the remaining candidates. We also derived strong limits on the unpulsed emission from PSRs B1046−58, B1055−52 and B1610−50.

These data argue strongly that the proposed ring-shaped X-ray nebula and associated radio nebula around PSR B1055−52 are in fact due to emission from background sources. A lack of a nebula associated with PSR B1055−52 combined with its observed high energy characteristics indicates that it probably converts most of its spin-down energy into high energy emission and not a relativistic wind. The lack of a nebular associated with PSR B1610−50 clearly shows that it is not moving sufficiently fast to be associated with Kes 32. PSR J1105−6107 is located near the edge of a thermal region which will make identification of any radio PWN difficult.

If the undetected nebulae around all our candidate pulsars are compact, then these pulsars convert less than 10^{-6} of their spin-down energy into radio emission. Alternatively, assuming that PSR B1046−58 and PSR B1610−50 have similar winds to PSR B1757–24 and PSR B1853+01 we derive a maximum ISM number density for PSR B1046−58 and PSR B1610−50 of $n_0 \lesssim 2.2 \times 10^{-3}\,\mathrm{cm}^{-3}$ and $n_0 \lesssim 1 \times 10^{-2}\,\mathrm{cm}^{-3}$, respectively. The low-density is supported by the lack of any potential parental SNRs associated with these young pulsars. We also constrain their spatial velocities to be less than $\sim 450\,\mathrm{km}\,s^{-1}$.

Our failure to detect nebulae around the young, and very energetic pulsars PSR B1046−58 and PSR B1610−50 indicates that a high spin-down rate is insufficient to generate a PWN. When combined with the very faint nebulae we did detect associated with the somewhat less energetic PSR B0906–49 these results highlight the role that the ISM plays in the production of such nebulae. The sensitivity limits achieved here would be unattainable without the use of pulsar gating and we now plan to employ this facility on the VLA to search a larger sample of pulsars. Such a sample will not only provide vital data on the wind parameters of a varied range of pulsars but will also supply valuable information on the ISM.

ACKNOWLEDGMENTS

We would like to thank Dale Frail for valuable discussions during the preparation of this work, Shinpei Shibata for providing the ASCA image of PSR B1055−52 and Dick Manchester for supplying the pulsar ephemerides. The Australia Telescope is funded by the Commonwealth of Australia for operation as a National Facility managed by CSIRO. The MOST is operated by the University of Sydney with support from the Australian Research Council and the Science Foundation for Physics within the University of Sydney. BMG acknowledges the support of an Australian Postgraduate Award, and of NASA through Hubble Fellowship grant HF-01107-01-98A awarded by the Space Telescope Science Institute, which is operated by the Association of Universities for Research in Astronomy, Inc., for NASA under contract NAS 5–26555.

REFERENCES

Arons J., 1993, ApJ, 408, 160
Becker W., Trümper J., 1997, AA, 326, 682
Becker W., 1998, in The relationship between NSs and SNRs. Osservatorio Astrofisico Di Arcetri, Elba, http://www.arcetri.astro.it/∼elba98/
Bell J. F., Bailes M., Bessell M. S., 1993, Nat, 364, 603
Blandford R. D., Ostriker J. P., Pacini F., Rees M. J., 1973, JA&A, 23, 145
Caraveo P. A., 1993, ApJ, 415, L111
Cheng A. F., Helfand D. J., 1983, ApJ, 271, 271
Clark B. G., 1980, AA, 89, 377
Cohen N. L., Cotton W. D., Geldzahler B. J., Marcaide J. M., 1983, ApJ, 264, 273
Combi J. A., Romero G. E., Azcárate I. N., 1997, Astrophys. Space Sci., 250, 1
Cordes J. M., 1996, in Johnston S., Walker M. A., Bailes M., eds, Pulsars: Problems and Progress, IAU Colloquium 160. Astronomical Society of the Pacific, San Francisco, p. 393
Cowie L. L., Hu E. M., Taylor W., York D. G., 1981, ApJ, 250, L25
Fierro J. M., 1995, PhD thesis, Stanford University
Frail D. A., Kulkarni S. R., 1991, Nat, 352, 785
Frail D. A., Scharringhausen B. R., 1997, ApJ, 480, 364
Frail D. A., Giacani E. B., Goss W. M., Dubner G., 1996, ApJ, 464, L165
Frater R. H., Brooks J. W., Whiteoak J. B., 1992, J. Electr. Electron. Eng. Aust., 12, 103
Gaensler B. M., Johnston S., 1995, Proc. Astr. Soc. Aust., 12, 76
Gaensler B. M., Stappers B. W., Frail D. A., Johnston S., 1998, ApJ, 499, L69
Gotthelf E. V., Kaspi V. M., 1998, ApJ, 497, L29
Green A. J., Cram L. E., Large M. I., Ye T.-S., 1999, ApJS, in press
Hankins T. H., Moffett D. A., Novikov A., Popov M., 1997, ApJ, 417, 735
Hansen B., Phinney E. S., 1997, MNRAS, 291, 569
Haslam C. G. T., Klein U., Salter C. J., Stoffel H., Wilson W. E., Cleary M. N., Cooke D. J., Thomasson P., 1981, AA, 100, 209
Johnston S., Lyne A. G., Manchester R. N., Kniffen D. A., D'Amico N., Lim J., Ashworth M., 1992, MNRAS, 255, 401
Johnston S., Manchester R. N., Lyne A. G., Kaspi V. M., D'Amico N., 1995, AA, 293, 795
Johnston S., Koribalski B. S., Weisberg J., Wilson W., 1996, MNRAS, 279, 661
Kafatos M., Sofia S., Bruhweiler F., Gull S., 1980, ApJ, 242, 294
Kaspi V. M., Bailes M., Manchester R. N., Stappers B. W., Sandhu J. S., Navarro J., D'Amico N., 1997, ApJ, 485, 820
Kaspi V. M., Lackey J. R., Pivovaroff M. J., Mattox J. R., Gotthelf E. V., Manchester R. N., Bailes M., Pace R., 1998, in The relationship between NSs and SNRs. Osservatorio Astrofisico Di Arcetri, Elba, http://www.arcetri.astro.it/∼elba98/
Kawai N., Tamura K., 1996, in Johnston S., Walker M. A., Bailes M., eds, Pulsars: Problems and Progress, IAU Colloquium 160. Astronomical Society of the Pacific, San Francisco, p. 367
Kawai N., Tamura K., Saito Y., 1998, Adv. Space Res., 21, 213
Kennel C. F., Coroniti F. V., 1984, ApJ, 283, 710
Kulkarni S. R., Hester J. J., 1988, Nat, 335, 801
Kulkarni S. R., Phinney E. S., Evans C. R., Hasinger G., 1992, Nat, 359, 300
McKee C. F., Ostriker J. P., 1977, ApJ, 218, 148
Michel F. C., 1982, Rev. Mod. Phys., 54, 1
Mignani R., Caraveo P. A., Bignami G. F., 1997, ApJ, 474, L51
Nel H. I. et al., 1996, ApJ, 465, 898
Ögelman H., Finley J. P., 1993, ApJ, 413, L31
Rees M. J., Gunn J. E., 1974, MNRAS, 167, 1
Reynolds J. E., 1994, ATNF Technical Document Series, 39.3040
Robertson J. G., 1991, Aust. J. Phys., 44, 729
Sault R. J., Killeen N. E. B., 1998, The Miriad User's Guide. Australia Telescope National Facility, Sydney, (http://www.atnf.csiro.au/computing/software/miriad/)

Shibata S. et al., 1997, ApJ, 483, 843
Taylor J. H., Cordes J. M., 1993, ApJ, 411, 674
Taylor J. H., Manchester R. N., Lyne A. G., Camilo F. 1995. Unpublished (available at ftp://pulsar.princeton.edu/pub/catalog)
Thompson D. J. et al., 1999, ApJ, accepted, astro-ph/9811219
Wang Q. D., Li Z.-Y., Begelman M. C., 1993, Nat, 364, 127
Weiler K. W., Panagia N., 1978, AA, 70, 419